ISBN: 978-3-95450-179-3 doi:10.18429/JACoW-FEL2017-MOP019

TRANSIENT THERMAL STRESS WAVE ANALYSIS OF A THIN DIAMOND CRYSTAL UNDER LASER HEAT LOAD*

Bo Yang†, Department of Mechanical & Aerospace Engineering, University of Texas at Arlington, Arlington, TX 76019, USA
Juhao Wu‡, SLAC National Accelerator Laboratory, Menlo Park, California, 94025, USA

Abstract

When a laser pulse impinges on a thin crystal, energy is deposited resulting in an instantaneous temperature surge in the local volume and emission of stress waves. In the present work, we perform a transient thermal stress wave analysis of a diamond layer 200 µm thick in the low energy deposition per pulse regime. The layer thickness and laser spot size are comparable. The analysis reveals the characteristic non-planar stress wave propagation. The stress wave emission lasts by hundreds of nanoseconds, at a time scale relevant to the high-repetition-rate FELs at the megahertz range. The kinetic energy converted from the thermal strain energy is calculated, which may be important to estimate the vibrational amplitude of the thin crystal when excited under repeated heat loads. The transient heat transfer plays an important role in draining the mechanical energy during the dynamic wave emission process.

INTRODUCTION

Thin crystals play an important role in enabling X-ray FELs of high peak-brightness, Angstrom wavelengths, and femtosecond/sub-femtosecond pulse durations [1]. They are used as monochromator for self-seeding [2,3] and one-shot spectrometer [4-6], for example. To function properly, they must be able to sustain the ever-increasing heat load, especially from multiple pulses at high repetition rates. When a high-intensity light pulse strikes a crystal, energy is deposited through photon-electron interaction. The energy is further passed on to the lattice. It results in a temperature surge over the volume on its way of passage. It is speculated that the deposited thermal strain energy would trigger stress waves. The dynamic strain field may directly affect the optics performance. The stress wave emission may also convert a part of the deformation energy into kinetic energy. When cumulated near a resonant frequency, it may lead to severe vibration impairing the device steadiness.

In the present work, we perform a transient thermal stress wave analysis to elucidate the dynamics of stress wave emission in a thin diamond crystal under heat load of an X-ray FEL pulse. The equation of motion and the equation of energy conservation are solved together for both transient stress wave propagation and transient heat transfer. Although the mechanical deformation process does not affect much the heat transfer process, their coupling is important to reveal how the initial thermal strain energy is relaxed, i.e., partially to the kinetic energy, and partially back to the thermal energy. The case from Ref. 7 is (re-)examined. The diamond crystal thickness is 200 µm. The laser spot size is about twice the thickness. The absorption rate is adjusted such that the initial temperature rise is less than 2 K at the center of the Gaussian beam, in the low energy deposition regime. The problem is numerically solved by applying a finite volume method. The analysis reveals the characteristic non-planar stress wave propagation. While the deformation energy stored in the radial normal strain component is released in part through radial longitudinal and surface stress waves, that stored in the through-thickness normal strain component is depleted by emitting radial longitudinal stress waves due to Poisson's effect. This latter emission process lasts by hundreds of nanoseconds, at a time scale relevant to the high-repetition-rate FELs at the megahertz range. The resulting kinetic energy is calculated, which may be important to estimate the vibrational amplitude of the thin crystal when excited under repeated heat loads. The transient heat transfer plays an important role in draining the mechanical energy during the dynamic thermal stress wave emission process.

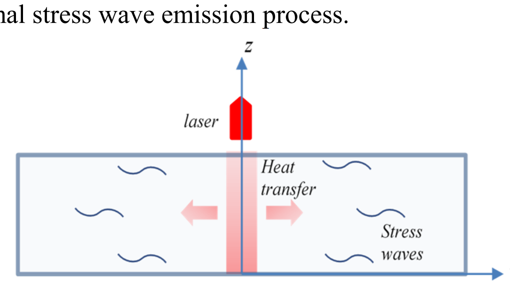

Figure 1: Schematic showing instantaneous heating and subsequent stress wave emission and heat transfer upon laser energy deposition in a thin crystal layer. The cylindrical coordinate system with axisymmetry is established.

PROBLEM FORMULATION

Consider an X-ray FEL impinging on a thin crystal, as schematically shown in Fig. 1. It interacts with the electrons and deposits a part of its energy first onto the electrons [8]. Later the energy is transferred to the lattice raising the local temperature. Then, the thermalized lattice expands dynamically emitting stress waves. The thermal diffusion begins at the same time. We aim to analyse the process of transient thermal stress wave emission. A cylindrical coordinate system (r, θ, z) is established with z-axis normal to the crystal surface. Only a laser beam perpendicular to the crystal surface is considered.

* Work supported by the US Department of Energy (DOE) under contract DE-AC02-76SF00515 and the US DOE Office of Science Early Career Research Program grant FWP-2013-SLAC-100164.
† boyang@uta.edu
‡ jhwu@slac.stanford.edu

ISBN: 978-3-95450-179-3 doi:10.18429/JACoW-FEL2017-MOP019

The equation of motion in the absence of body forces is given by:

$$\rho\frac{dv}{dt} = \nabla\cdot\boldsymbol{\sigma}, \tag{1}$$

where ρ is the mass density, $\boldsymbol{v}(= d\boldsymbol{u}/dt)$ is the velocity, $\boldsymbol{u}$ is the displacement, $\boldsymbol{\sigma}$ is the stress tensor, and t is time. Assuming the isotropic thermoelasticity, the constitutive law is given by:

$$\boldsymbol{\sigma} = 2G\left(\boldsymbol{\varepsilon} - \tfrac{1}{3}\mathrm{tr}(\boldsymbol{\varepsilon})\boldsymbol{I}\right) + 3K_b\left(\tfrac{1}{3}\mathrm{tr}(\boldsymbol{\varepsilon}) - \varepsilon_T\right)\boldsymbol{I}, \tag{2}$$

where G is the modulus of rigidity, K_b is the bulk modulus, $\boldsymbol{\varepsilon}$ is the strain tensor, ε_T is the thermal strain, $\boldsymbol{I}$ is the identity matrix, and $\mathrm{tr}(\boldsymbol{\varepsilon})$ denotes the trace of $\boldsymbol{\varepsilon}$.

The equation of energy conservation is given by:

$$\frac{d(U_T+U_\varepsilon)}{dt} = -\nabla\cdot(-\kappa\nabla T) + \boldsymbol{\sigma}:\nabla\boldsymbol{v}, \tag{3}$$

where T is the temperature, $U_T(=\int\rho C_v dT)$ is the thermal energy density, $U_\varepsilon(=(1/2)\boldsymbol{\sigma}:(\boldsymbol{\varepsilon}-\varepsilon_T\boldsymbol{I}))$ is the elastic strain energy density, κ is the thermal conductivity, C_v is the specific heat. On the right-hand side, the first term is the heat transfer according to Fourier's law. The second term is the rate of work done by the stress through a velocity field.

The initial displacement and velocity fields are both set equal to zero: $\boldsymbol{u}_0 = 0$, and $\boldsymbol{v}_0 = 0$. The initial temperature field is set at $T_0 = 300$ K. Upon a Gaussian laser pulse, the laser energy is partially absorbed raising the temperature on the way of its passage. The change of thermal energy density as a function of r and z is given by:

$$\Delta U_T(r,z) = \frac{2I_0}{\pi a^2 L}e^{-\frac{2r^2}{a^2}}e^{-\frac{z}{L}}, \tag{4}$$

where I_0 is the laser pulse energy, a is the transverse FWHM of the Gaussian beam along the radial direction, and L is the attenuation length. The corresponding temperature increase is determined from the relationship of U_T to T, which is generally a nonlinear function.

At the plate edge boundary, the fixed boundary condition is applied. The temperature is held at 300 K at all times.

In the following study, since the heat load is low, the material parameters are all nearly constant. Yet, the general nonlinear properties, including the thermal strain and specific heat [9] and the thermal conductivity [10], are used. One may refer to Ref. 11 for the details.

RESULTS AND DISCUSSION

Simulation was run for transient thermal stress wave analysis with thickness h = 200 µm, laser spot size a = 350 µm, and plate radius = 1.5 mm. Only a single pulse input is examined, with pulse energy I_0 = 70 µJ and attenuation length L = 380 µm [7]. Fiftty-one equal divisions are used to discretize the domain in the thickness direction. An adaptive mesh is used in the radial direction. 70 equal divisions are used in near 175 µm distance, and 300 unequal divisions with increasing size by gradient 1.003 in following 1325 µm distance. The time step is 0.1 ns. The stress waves would propagate by < 2 µm in space each time step, smaller than the spatial grid size. Since we use an implicit finite difference scheme for time integration, the solution is unconditionally stable. The simulation is terminated at t = 400 ns. Selected results are plotted in Figs. 2–4.

Figure 2 shows some snap shots of the fields at t = 1, 5, 10, 20, and 60 ns. In the left column (a)–(e), the 3D surface plot is used to show velocity component v_z, and the contour plot with a color code at the base to indicate strain component ε_{zz}. In the right column, correspondingly velocity component v_r, and strain component ε_{rr} are shown. Figure 3 shows the time histories of the total deformation energy, $\int_V U_\varepsilon\, dV$, the total kinetic energy $\int_V \frac{1}{2}\rho\boldsymbol{v}\cdot\boldsymbol{v}dV$, and the change of thermal energy, $\int_V (U_T - U_{T0})\,dV$, where V is the domain and U_{T0} is the initial thermal energy density upon the laser energy deposition. The r- and z-components of kinetic energy, $\int_V \frac{1}{2}\rho v_r^2 dV$ and $\int_V \frac{1}{2}\rho v_z^2 dV$, are also calculated, which represents the wave activity in the two corresponding directions, respectively. Figure 4 shows the time evolution of temperature at three different radial distances r = 0, 175 and 350 µm on the front and back surfaces

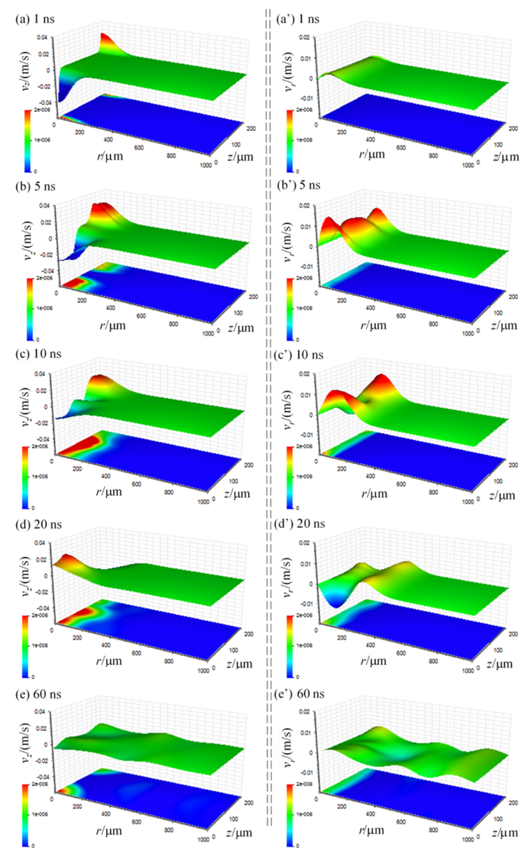

Figure 2: Snapshots of stress wave emission at various moments: (a,a') 1 ns; (b,b') 5 ns; (c,c') 10 ns; (d,d') 20 ns; (e,e') 60 ns. In the left column, the 3D profiles show the field of velocity component v_z, and the contour plots with a color code at the base indicate the field of strain component ε_{zz}. In the right column, correspondingly velocity component v_r, and strain component ε_{rr} are shown.

ISBN: 978-3-95450-179-3 doi:10.18429/JACoW-FEL2017-MOP019

$z = 0$ and 200 μm. At $r = 350$ μm, the temperature change is trivial up to the time of 400 ns calculated.

In this case, about 41 % of the laser energy, i.e., 28.6 μJ out of 70 μJ, is deposited into the diamond. Since it is over a relatively large area, the maximum temperature increase at the center of entry surface is only 1.83 K. Correspondingly, the wave fields are of low magnitude. Although the magnitudes are small, the characteristics of the transient heat transfer and stress wave emission are similar to those observed in a much concentrated case [11].

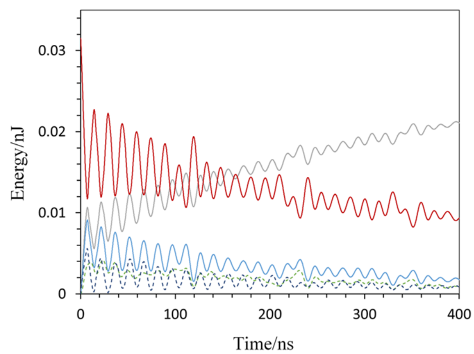

Figure 3: Time histories of thermal energy change (grey solid), deformation energy (red solid), and total (blue solid), r-portion (green dashed) and z-portion (purple dashed) of kinetic energy in a diamond plate upon a single-pulse laser input.

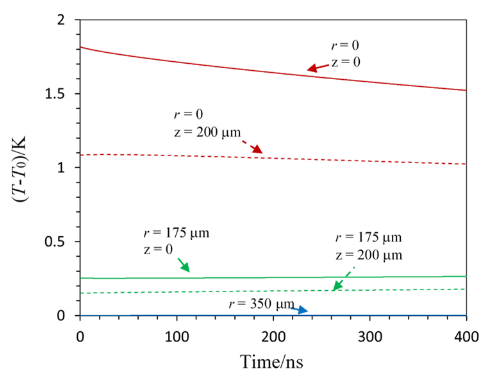

Figure 4. Time histories of temperature at three different distance r = 0, 175, 350 μm on the front surface (z = 0, solid) and back surface (z = 200 μm, dashed) in a diamond plate upon a single-pulse laser input.

As seen in Fig. 2, the radial thermal strain component triggers radial dilatational waves and Rayleigh surface waves radiating away from the center. In contrast, the wave activity due to the transverse thermal strain component is much more complicated. First, this component of thermal strain induces through-thickness longitudinal stress waves bouncing back and forth between the surfaces. Second, since the heated zone is finite, this mode of wave propagation experiences constraint of particles still cool at the boundary. Due to Poisson's effect, the dynamic transverse normal straining (i.e., a breathing mode) induces compression and tension in the radial direction, emitting radial longitudinal stress waves. This is the main mechanism depleting the energy stored in the transverse normal strain component away from the heated site. The bumps following the front wave in Fig. 2(e') are due to this mechanism.

The oscillation of an energy term in Fig. 3 is due to the transverse wave activity. Since the diamond layer is thick compared to the lateral size, the waves have reached the boundary and been reflected a few times during the period of time calculated, as seen roughly every 110 ns in Fig. 3. After 400 ns, the temperature in the center of the hot zone has dropped by about 15 %. Importantly, it is seen in Fig. 3 that a significant portion of the mechanical energy is being converted back to thermal energy. Only a small part is converted to kinetic energy, which however, if cumulated, may cause vibrational problem when the layer is excited.

SUMMARY

An exemplary case of a thin diamond layer 200 μm thick is analysed in the low energy deposition per pulse regime. The laser spot size to thickness ratio is roughly 2:1. It reveals the characteristic non-planar stress wave propagation. While the deformation energy stored in the radial normal strain component is radiated through radial longitudinal and surface stress waves, that stored in the through-thickness normal strain component is depleted in a much more complicated way. While the corresponding longitudinal stress waves bounce back and forth between the layer surfaces, they induce radial longitudinal stress waves according to Poisson's effect. Depending on the laser spot size to thickness ratio, this emission process can last a long time, for instance, hundreds of nanoseconds in the analysed case, at a time scale relevant to the high-repetition-rate FEL at the megahertz range. The transient heat transfer is found to play an important role in draining the mechanical energy during the thermal stress wave process. The resulting kinetic energy is calculated, which may be important to estimate the vibrational amplitude of the thin crystal when excited under repeated heat load.

REFERENCES

[1] Shvyd'ko, Y., Blank, V. and Terentyev, S., "Diamond x-ray optics: transparent, resilient, high-resolution, and wavefront preserving," *MRS Bulletin* **42**, 437-444 (2017).

[2] Geloni, G., Kocharyan, V. and Saldin, E., "A novel self-seeding scheme for hard X-ray FELs," *Journal of Modern Optics* **58**, 1391-1403 (2011).

[3] Amann, J. *et al.*, "Demonstration of self-seeding in a hard-X-ray free-electron laser," *Nature Photonics* **6**, 693-698 (2012).

[4] Yabashi, M. *et al.*, "Single-shot spectrometry for X-ray free-electron lasers," *Physical Review Letters* **97**, 084802 (2006).

[5] Zhu, D. *et al.*, "A single-shot transmissive spectrometer for hard X-ray free electron lasers," *Applied Physics Letters* **101**, 034103 (2012).

ISBN: 978-3-95450-179-3 doi:10.18429/JACoW-FEL2017-MOP019

[6] Rehanek, J. *et al.,* "The hard X-ray photon single-shot spectrometer of SwissFEL—initial characterization," *Journal of Instrumentation* **12**, A07001 (2017).

[7] Stoupin, S. *et al.,* "Direct observation of dynamics of thermal expansion using pump-probe high-energy-resolution x-ray diffraction," *Physical Review B* **86**, 054301 (2012).

[8] Von der Linde, D., Sokolowski-Tinten, K. and Bialkowski, J., "Laser–solid interaction in the femtosecond time regime," *Applied Surface Science* **109**, 1-10 (1997).

[9] Reeber, R. R. and Wang, K., "Thermal expansion, molar volume and specific heat of diamond from 0 to 3000K," *Journal of Electronic Materials* **25**, 63-67 (1996).

[10] Wei, L., Kuo, P., Thomas, R., Anthony, T. and Banholzer, W., "Thermal conductivity of isotopically modified single crystal diamond," *Physical Review Letters* **70**, 3764 (1993).

[11] Yang, B., Wang, S. and Wu, J., "Transient thermal stress wave and vibrational analyses of a thin diamond crystal for X-ray FELs under high repetition-rate operation," *Journal of Synchrotron Radiation* (under review).